147. Inhibition of Electron-Hole Recombination in Substitutionally Doped Colloidal Semiconductor Crystallites

by **Jacques Moser** and **Michael Grätzel***

Institut de Chimie Physique, Ecole Polytechnique Fédérale, CH–1015 Lausanne

and **Roland Gallay**

Institut de Physique Expérimentale, Ecole Polytechnique Fédérale, CH–1015 Lausanne

(16.VII.87)

The substitutional doping of 120-Å-sized TiO_2 particles with Fe(III) ions has a profound effect on the charge carrier recombination time in this colloidal semiconductor. In undoped particles, the mean lifetime of an electron-hole pair is *ca.* 30 ± 15 ns. Doping with 0.5% Fe(III) drastically augments the charge-carrier lifetime which is extended to minutes or hours. The slow caracter of the recombination dynamics in Fe(III)-doped colloids was confirmed by laser photolysis using the characteristic optical absorption of electrons in TiO_2 to monitor the time course of the reaction. EPR studies showed the Fe(III) ions to enter the host lattice on Ti(IV) sites, charge compensation taking place through the formation of oxygen vacancies. Valence-band holes produced under band-gap excitation react with these centers in the bulk forming Fe(IV), the conduction band electrons being trapped by Ti(IV) at the particle surface. Presumably, the spatial separation of the trapped electron and hole sites inhibits their recombination.

Introduction. – The recombination of holes and electrons is an important electronic process in semiconductors. Rectification, photoconductivity, and transistor behavior are all critically dependent on the life-time of the injected mobile carriers. The recombination rate plays also a crucial role in photocatalytic reactions with semiconductor particles, in particular the conversion of solar light energy into fuels [1].

We have recently performed a direct analysis of the dynamics of charge-carrier trapping and recombination in TiO_2 colloids [2]. The mean lifetime of a single electron-hole pair in the 120-Å-sized particles was found to be 30 ns. We extend now these investigations to doped TiO_2 colloids and report on the discovery of a striking retardation in the charge-carrier recombination rate induced by introducing small levels of Fe(III) dopant in the TiO_2 lattice. These effects are further elucidated by EPR studies. A mechanism for the inhibition of electron-hole recombination is proposed.

Experimental. – *Preparation and Characterization of Colloidal TiO_2 Doped with Fe(III)*: $TiCl_4$ (*Fluka, puriss.*) was further purified by vacuum distillation (40°, *ca.* 25 Torr) until a colorless liquid was obtained. The purified material (5 g) was slowly added to 0.2 l H_2O at 0°. The final pH of the soln. was between 0.5 and 1. At this time, the required amount of $FeCl_3 \times H_2O$ (*Fluka, puriss.*) was added to give a doping level between 0.05 and 2 atomic percent. In most cases, the dopant concentration was 0.5%, which is well within the solubility limit of Fe(III) in TiO_2, and which gave excellent charge separation effects. The yellow soln. was dialyzed for 1 h against a $FeCl_3$ soln. of the same composition. Subsequently, the mixture was dialyzed against pure H_2O until the pH of the colloidal soln. was about 3. During dialysis, the characteristic brown/yellow color of the Fe(III) aqua ions disappeared indicating that the Fe(III) entered the TiO_2 lattice. This was confirmed quantitatively by elemental analysis of the colloidal particles performed after evaporation of the H_2O in a rotavap at 40°, followed by washing and drying at 100°. The carbon content of the doped TiO_2 was also analyzed and was found to be 0.12%.

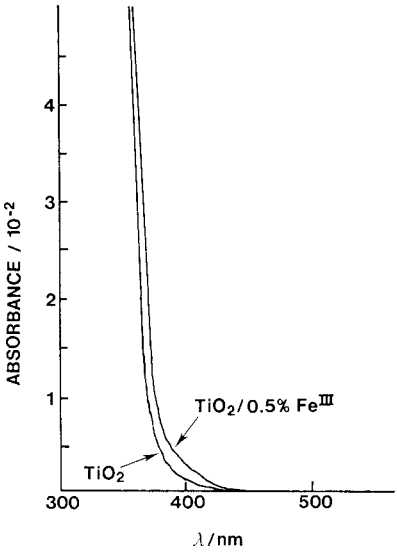

Fig. 1. *Absorption spectrum of a TiO_2 colloid and a Fe(III)-doped TiO_2 colloid in H_2O.* TiO_2 concentration 7 g/l.

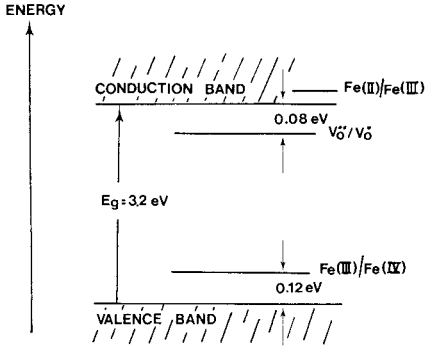

Fig. 2. *Energy-level diagram for Fe(III)-doped anatase.* Note that the Fe^{III}/Fe^{II} redox level is in the conduction band.

Electron and X-ray diffraction of the doped TiO_2 colloid showed it to consist of a mixture of anatase and an amorphous phase. No trace of rutile or any other phases could be detected. The mean particle radius was determined by quasielastic light scattering technique as 17 nm.

The UV/VIS absorption spectrum of the sol is shown in *Fig. 1*. The absorption edge of the Fe(III) doped sample is red-shifted by *ca.* 20 nm with respect to Fe-free TiO_2. A similar red shift has been observed with iron-doped single crystals of rutile [3] [4]. The shift has been attributed to the excitation of 3d-electrons of the Fe(III) to the TiO_2 conduction band. The energy level for the redox transition of substitutional Fe(III) to Fe(IV) in rutile is shown in *Fig. 2*. According to *Mizushima et al.* [4], this level is located 3 eV below the conduction band edge which would place the onset of the optical absorption at 415 nm, in good agreement with the experimental observation.

Laser-photolysis experiments were carried out with a Q-switched frequency-tripled Nd-YAG laser (*JK 2000*) having a pulse width at half maximum of 15 ns. This was combined with transient spectroscopy and a data acquisition system developed by Dr. *P. P. Infelta* in our laboratory. Continuous illuminations employed a 100-ml photochemical quartz reactor (*Applied Photophysics*) equipped with an immersion 150-W medium-pressure Hg lamp surrounded by a circulating water filter. Prior and during irradiation, solns. were degassed by N_2 bubbling.

EPR studies employed a *E-102-Varian* spectrometer at 9.2 GHz. Microwave frequencies were measured with a *Hewlett-Packard* frequency counter. Magnetic field determination was carried out with a *Varian* KCl standard (3×10^{14} centers) and a *Bruker* NMR probe. Band-gap excitation of the colloidal TiO_2 particles was carried out at r.t. outside the spectrometer by focussing the output of a 150-W high-pressure Hg lamp onto the sol contained in a cylindrical quartz tube with a diameter of 4 mm.

Results. – *Laser Photolysis Experiments. Fig. 3* illustrates the effect of Fe(III) doping on the kinetics of charge-carrier recombination in colloidal TiO_2 particles. The colloidal semiconductor is excited by the 355-nm laser pulse producing electron-hole pairs. Trapping of the electrons by surface TiO_2 ions takes place within a few picoseconds [2]. The trapped electrons have a characteristic blue color, the spectral maximum in acidic solution being at 620 nm with an extinction coefficient of $1200 M^{-1} cm^{-1}$ [5]. The electron

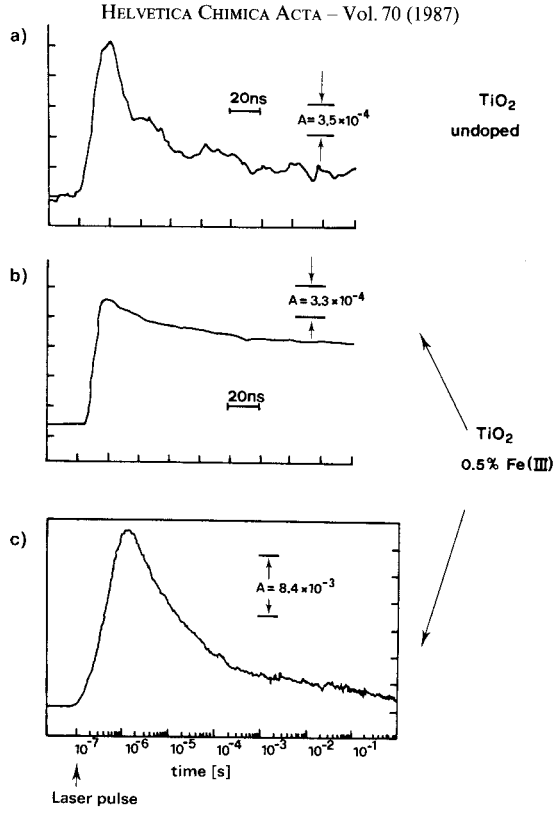

Fig. 3. *Effect of Fe(III) doping of colloidal TiO_2 on the dynamics of electron-hole recombination.* The 800-nm absorption of trapped electrons is used to monitor the recombination kinetics after 355-nm laser excitation of the colloidal particles. Conditions: $[TiO_2]$ = 3 g/l for undoped particles; $[TiO_2]$ = 7 g/l for doped particles; colloidal solutions are deaerated with Ar.

absorption in the red is recorded as a function of time. in *Fig. 3*, the electron decay is observed at 800 nm where the extinction coefficient is $800 M^{-1}$ cm^{-1}. *Fig. 3a* refers to undoped TiO_2 (particle concentration 1.8×10^{-7} M, diameter 12 nm) and an initial average concentration of 1.3 electron-hole pairs per particle. The decay of the 800 nm absorption is here very fast, in agreement with earlier observations [2] where the mean lifetime of a single electron-hole pair in these particles was determined as (30 ± 15) ns.

A striking retardation of the electron decay is observed upon introducing 0.5% Fe(III) in the lattice of the colloid. In *Fig. 3b*, the concentration of TiO_2 particles is 1.2×10^{-6} M (particle diameter 17 nm), and 2.8 electron-hole pairs per particle were present initially after laser excitation. In contrast to the undoped particles, only a small fraction of the electron absorption decays away within 200 ns. In *Fig. 3c*, the recombination dynamics in the doped TiO_2 colloid are re-examined on a logarithmic time scale. Here, the average number of electron-hole pairs calculated from the transient absorbance immediately after the laser pulse was 146 per semiconductor particle. The 800-nm absorption decay extends over a surprisingly long time. Even a second after laser excitation, a fraction of *ca.* 10% of the electron absorption persists showing that the charge-carrier recombination is drastically retarded.

The transient spectrum obtained with the Fe(III)-doped TiO_2 particles from the absorbance change immediately after the laser pulse is shown in *Fig. 4*. It differs from the transient spectrum of Fe(III)-free colloid [5] in as much as the maximum is at 420 nm instead of 620 nm. Based on spectral data obtained previously with Fe-doped single crystals [3] or powders [6] of TiO_2, the feature at 420 nm is identified as substitutional Fe(IV) formed by the reaction of TiO_2 valence-band holes with the Fe(III) centers. The absorption in the red part of the spectrum is attributed to electrons trapped at Ti^{4+}-surface sites. These assignments are confirmed by EPR results reported below.

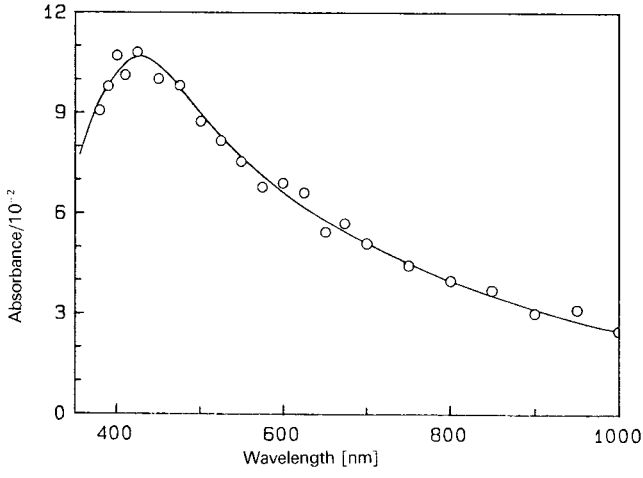

Fig. 4. *Transient spectrum obtained immediately after 355-nm laser excitation of colloidal TiO_2 particles doped with 0.5% Fe(III).* Conditions: optical pathlength 0.5 cm; $[TiO_2]$ = 7 g/l; solutions deaerated with Ar.

EPR Experiments with Fe(III)-Doped Colloidal TiO_2 Particles. The EPR spectrum of a TiO_2 colloid doped with 0.5% Fe(III) is given in *Fig. 5a*. It contains two features with g values of 4.295 and 2.0023. Based on the work of *Gainon* and *Lacroix* [7], and *Horn* and *Schwerdfeger* [8] with Fe(III)-doped single crystals of anatase, the two signals are assigned to Fe(III) on Ti(IV)-lattice site with and without charge compensation by an oxygen vacancy at a nearest neighbor site, respectively. For electroneutrality reasons, the number of oxygen vacancies generated by iron doping corresponds to half of that of substitutional Fe(III):

$$Fe_2O_3 \rightarrow 2\,Fe_{Ti}^{III\prime} + V_o^{\bullet\bullet} + 3O_o \qquad (1)$$

Thus, part of the Fe_{Ti}^{III} centers have a full coordination sphere of lattice oxygen anions while the rest, *i.e.* the charge-compensated centers Fe_{cc}^{III}, have an oxygen vacancy at a nearest neighbor site. Uncompensated Fe_{Ti}^{III} have tetragonal symmetry, while for charge compensated centers the symmetry is lower. For both paramagnetic centers, we have calculated the powder spectrum using the spin-hamiltonian parameters given in *Table 1* of [8a]. The spin-hamiltonian was spatially averaged taking *Zeeman* and crystal-field interactions into account. In the case of Fe_{cc}^{III}, *Zeeman* term was treated as a first-order peturbation of the crystal field. The theoretical predictions are in agreement with the

spectrum in *Fig. 5a*, although several calculated components for the Fe^{III}_{cc} signal are not observed experimentally. This is explained [8] by the strong temperature and, likely, pressure dependency of zero-field splitting which leads to a broadening of this resonance line. From the width of the line of *ca.* 100 gauss, it can be inferred that the Fe centers are surrounded by crystalline and not amorphous TiO_2.

Fig. 5b shows the effect of band-gap irradiation on the EPR spectrum of the Fe(III)-doped colloid. The sample was irradiated with a high-pressure Hg lamp for several hours at room temperature. Subsequently, it was rapidly cooled to 77 K and the EPR spectrum recorded. The signal of charge-compensated Fe^{III} disappeared completely during illumination, and a new paramagnetic center appeared near that of Fe^{III}_{Ti} without charge compensation. The g values of this center $g_{\parallel} = 1.883$ and $g_{\perp} = 1.927$ correspond precisely to the signal produced by band-gap irradiation of undoped TiO_2 colloids [9] which has been identified with Ti^{3+} ions located at the particle surface. At 77 K, this signal remains

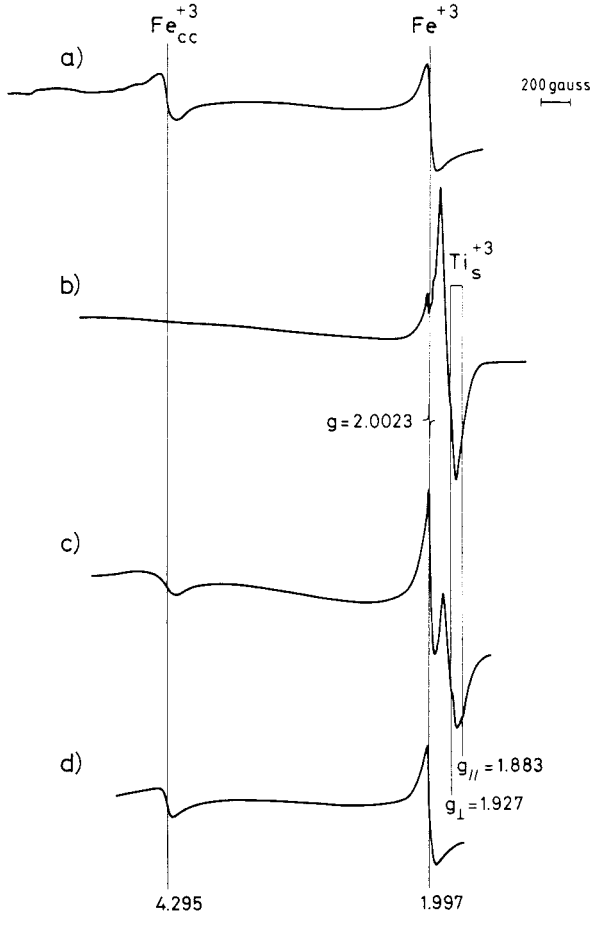

Fig. 5. *EPR spectra of Fe(III) doped colloidal TiO_2 particles in aqueous solution. a*) Prior to irradiation; *b*) after 18 h of illumination at room temperature; *c*) 0.5 h after the lamp has been turned off; *d*) 24 h after the lamp has been turned off. All spectra recorded at 77 K.

stable, while at room temperature it disappears slowly. The EPR spectra in *Figs. 5c* and *5d* were recorded after rewarming the irradiated colloid at room temperature for 0.5 and 24 h, respectively. The Ti^{3+} signal disappeared completely during this period, and the Fe(III) resonance lines reappeared. By comparing *Fig. 5a* with *5d*, one notices a slight increase in the Fe^{III}_{Ti} signal at the expense of that for Fe^{III}_{cc}.

Continuous-Photolysis Experiments. Concomitantly with the changes in the EPR spectrum reported in *Fig. 5*, one observes striking alterations in the color of the Fe(III)-doped TiO_2. Band-gap irradiation of deaerated colloids produces a grayish-green coloration of the TiO_2 particles. Such an irradiated sol displays a broad absorption band, the extinction increasing continuously from the IR towards the UV region (*Fig. 6*). The

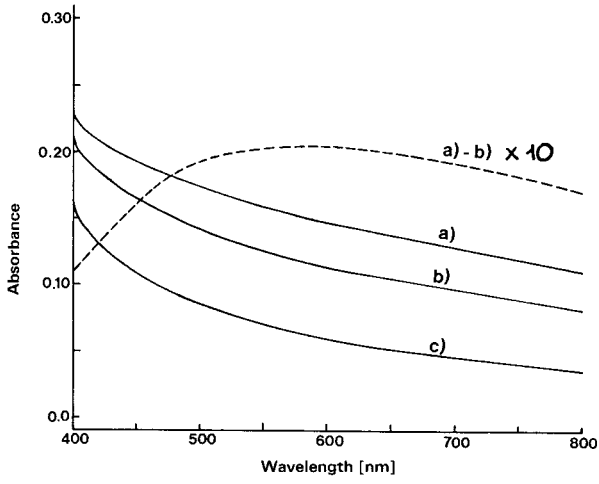

Fig. 6. *Absorption spectra of illuminated Fe(III)-doped TiO_2 colloids in aqueous solution. a*) After 10 h of irradiation of a N_2-purged solution with a medium-pressure Hg lamp; *b*) after admission of air to the irradiated sample; *c*) as *b*), after standing in the dark for 3 h; *a*)–*b*) difference spectrum between *a*) and *b*). Conditions: $[TiO_2]$ = 5 g/l, pH 2.7; doping level of Fe^{3+} is 0.1%.

features are similar to the transient spectrum obtained immediately after laser excitation of the colloidal particles. The maximum around 420 nm observed in *Fig. 4* is not resolved in *Fig. 6*. This is probably due to the overlapping band-gap absorption of the colloid. Curve *b* in *Fig. 6* was obtained after admission of air to the irradiated sample resulting in a color change from grayish-green to yellow. Substracting curve *b* from *a* yields the dashed line. This spectrum exhibits the typical features of absorption of surface trapped electrons in colloidal TiO_2 [5] [9].

Discussion. – The important finding of this work concerns the drastic retardation in the electron-hole recombination rate by doping TiO_2 semiconductor crystallites with small amounts of Fe(III). The EPR studies show the Fe(III) ions to enter the colloidal particles on Ti(IV) sites, charge compensation taking place through the formation of oxygen vacancies. According to the energy-level scheme presented in *Fig. 2*, these centers can act as shallow traps for the valence band holes produced under band-gap illumination:

$$h^+ + Fe^{III} \rightarrow Fe^{IV} \qquad (2)$$

The trapping of conduction-band electrons by substitutional Fe(III) can be excluded on energetic grounds. The Fe^{III}/Fe^{II} redox level is located in the conduction band of TiO_2 [4] rendering the reaction of e_{cb}^- with Fe(III) thermodynamically unfavorable.

Evidence for hole trapping by Fe(III) is provided by the EPR and laser-flash experiments. The EPR results in *Fig. 5* show the disappearance of the Fe(III) signal under illumination. Since the EPR signal from charge-compensated Fe(III) disappears first, these centers must have a higher cross section for hole scavenging than the uncompensated ones. The flash-photolysis results in *Fig. 4* show that the Fe(IV) absorption at 420 nm is already present at the end of the laser pulse. At a doping level of 0.5%, each TiO_2 particle contains on the average 371 Fe(III) centers. The scavenging of valence-band holes by these centers appears to occur within the 10-ns duration of the laser pulse.

The trapping of the conduction band electrons in colloidal TiO_2 particles is also a very rapid reaction which was shown to be completed in less than 40 ps [2]. Earlier EPR studies have identified the trapped electrons as Ti^{3+} ions located at the surface of the colloidal particles [9]. Thus, in the Fe(III)-doped TiO_2 system, both positive and negative mobile charge carriers are rapidly immobilized on trapping sites. Important for sustaining the light-induced charge separation is the fact that the two trapping sites are locally separated. Whereas the electrons are localized at the surface of the colloidal particles, the trapped hole states, *i.e.* the Fe(IV) centers are randomly distributed over the whole volume of the particle (*Fig. 7*). It is suggested that this local separation of the charge carriers is responsible for the inhibition of recombination.

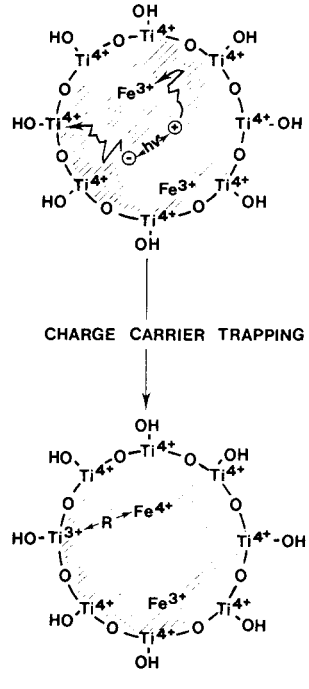

Fig. 7. *Schematic illustration of the mechanism proposed for light-induced charge separation in the Fe(III)-doped colloidal TiO_2 particles*

The recombination could occur *via* thermally assisted detrapping or electron tunnelling. Presently, the mechanism of the recombination process has not yet been ascertained, although the observation in *Fig. 3c* of a decay extending over many orders of magnitude in time would suggest that tunnelling makes a significant contribution. In such a case, the rate constant for recombination depends on the distance separating the electron-hole pair according to [10]:

$$k = \nu \exp(-2R/a_o) \tag{3}$$

where a_o is the radius of the hydrogenic wave function of the trapped carrier, and the frequency factor ν is proportional to the *Franck-Condon*-weighted density of states which depends on the exothermicity of the reaction. It reaches a maximum value of $10^{13\pm1}$ when the standard driving force $-\Delta_r G^*$ equals the free energy of reorganization λ. Since the charge carriers are immobilized in the traps, R becomes a function of reaction time. According to a model developed by *Inokuti* and *Hirayama* [11] and *Tachya* and *Mozumder* [12] for randomly oriented reactants, the survival probability of a reactant pair is given by [13]:

$$P(t) = \exp(-A(\ln^3(\nu t)) + h_1\ln^2(\nu t) + h_2\ln(\nu t) + h_3) \tag{4}$$

where A is related to the concentration of reactants and the meter a_o in *Eqn. 3*, and h_1, h_2, and h_3, are constants.

Eqn. 3 provides an explanation for the retardation of the electron-hole recombination in the Fe(III)-doped TiO_2 samples. As was shown above, a significant fraction of the trapped charge carriers survives even minutes after band-gap excitation. This can be rationalized in terms of the exponential decrease of the recombination probability with the distance separating the trapped electron and hole. A typical value for the reciprocal tunnelling length $2/a_o$ is 1.3 Å. Taking for υ the upper limit, *i.e.* 10^{14} s^{-1}, an electron trapped at a Ti(IV) surface site could within 1 s reach Fe(IV) centers located within 25 Å from the surface. Thus, for trapped electron-hole pairs which are in close vicinity, the recombination occurs rapidly, while for the centers that are further away, the tunnelling requires a much longer period.

While qualitatively instructive, *Eqn. 4* is inadequate to provide a quantitative description of the time course of charge-carrier recombination in the Fe(III)-doped TiO_2 samples such as shown in *Fig. 3c*. The assumptions used in the derivation of this equation, *i.e.* pseudo-first-order conditions for the acceptor or donor, infinite reaction volume, random distribution of reactants, and restriction of the reactive interaction to single pairs, are not applicable in the present case. A more adequate model taking into account the minute dimension of the reaction space of the colloidal particles as well as the nonhomogeneous spatial distribution of the trapped charge carriers is presently being developed and will be presented separately.

An important question, which will be finally addressed, concerns the mechanism of light-induced charge separation in the colloidal particles. It needs to be explained, why the electrons are trapped preferentially at Ti(IV) surface sites, if there are oxygen vacancies present in the bulk introduced by the Fe(III) doping, which are known to be excellent electron scavengers:

$$e^-_{cb} + V_o^{\bullet\bullet} \rightarrow V_o^{\bullet} \tag{5}$$

An electron trapped in an oxygen vacancy occupies a 1s orbital and hence should display a g value of 2.003. No such EPR signal was observed under illumination indicating that *Reaction 5* does not occur in the particles.

The following thermodynamic considerations are useful to rationalize these observations. In a semiconductor particle, the ratio of free conduction band electrons (N_{cb}) to the number of trapped ones (N_{tr}) is given by [14]:

$$\frac{N_{cb}}{N_{tr}} = \frac{Z}{2\,(n_{tr} - N_{tr})}\ \exp(-\varepsilon_{tr}/kT) \tag{6}$$

where n_{tr} is the number of traps per particle, Z is the translational partition function of the electrons in the conduction band, and ε_{tr} is the trap depth. In the case of 170-Å-sized TiO_2 particles, Z has the value 5.02×10^3 indicating that there are 1.06×10^4 thermally accessible conduction band states at room temperature.

Consider first electron trapping by oxygen vacancies. At a doping level of 0.5% Fe(III), there are 186 $V_o^{\bullet\bullet}$ centers in a TiO_2 particle. The energy of the $V_o^{\bullet\bullet}/V_o^{\bullet}$ level is 0.08 eV below the conduction band edge. Using *Eqn. 6*, one calculates that under the experimental conditions applied in *Fig. 3c*, where 146 conduction band electrons were produced by the laser pulse, only 50% of these electrons are trapped at equilibrium. The rest remains in the free state.

As for the electron trapping by Ti^{4+} surface states, one calculates that there are 1.03×10^4 of such states present in one 170-Å-sized TiO_2 particle using for the effective area of one Ti^{4+} ion a value of 8.78 Å^2. Since the trap depth of the Ti^{4+} centers is about the same as that for $V_o^{\bullet\bullet}$ [15], one derives from *Eqn. 6* that 99% of all the conduction-band electrons are trapped at the surface under the conditions applied in *Fig. 3c*. It is the increase in configurational entropy that favors surface with respect to bulk trapping.

This work was supported by the *Gas Research Institute*, Chicago, III., USA (subcontract with the *Solar Energy Research Institute*, Golden, Colorado) and the *Office Fédéral pour l'Energie* (Switzerland), and the *Fonds National Suisse de la Recherche scientifique*.

REFERENCES

[1] K. Kalyanasundaram, M. Grätzel, E. Pelizzetti, *Coord. Chem. Rev.* **1985**, *69*, 57.
[2] G. Rothenberger, J. Moser, M. Grätzel, N. Serpone, D.K. Sharma, *J. Am. Chem. Soc.* **1985**, *107*, 8054.
[3] B.W. Faughnan, Z.J. Kiss, *Phys. Rev. Lett.* **1968**, *21*, 1331.
[4] K. Mizushima, M. Tanaka, A. Asai, S. Iida, J.B. Goodenough, *J. Phys. Chem. Soc.* **1979**, *40*, 1129.
[5] U. Kölle, J. Moser, M. Grätzel, *Inorg. Chem.* **1985**, *24*, 2253.
[6] a) W.A. Weyl, T. Forland, *Ind. Eng. Chem.* **1950**, *42*, 257; b) W.M. Macverin, P.R. Ogle, *J. Am. Chem. Soc.* **1954**, *76*, 3846; c) F.K. McTaggart, J. Bear, *J. Appl. Chem.* **1955**, *5*, 643; d) J. Bear, F.K. McTaggart, *ibid.* **1958**, *5*, 72.
[7] D. Gainon, R. Lacroix, *Proc. Phys. Soc. (London)* **1962**, *79*, 658.
[8] a) M. Horn, C.F. Schwerdfeger, *Solid State Commun.* **1970**, *8*, 1741; b) M. Horn, C.F. Schwerdfeger, *J. Phys. Chem. Soc.* **1971**, *32*, 2529.
[9] R. Howe, M. Grätzel, *J. Phys. Chem.* **1985**, *89*, 4495.
[10] M. Grätzel, 'Heterogeneous Photochemical Electron Transfer Reactions', CRC Press, Boca Raton, Florida, USA, 1987.
[11] M. Inokuti, F. Hirayama, *J. Chem. Phys.* **1965**, *43*, 1978.
[12] M. Tachya, A. Mozumder, *Chem. Phys. Lett.* **1974**, *28*, 87.
[13] B.H. Milosavljevic, J.K. Thomas, *J. Phys. Chem.* **1985**, *89*, 1830.
[14] J.W. Mitchell, *Phot. Sci. Eng.* **1983**, *27*, 96.
[15] A.K. Gosh, R.B. Laver, R.R. Addiss, *Phys. Rev. B* **1973**, *8*, 4842.